A robust graph based framework for building precise maps from laser range scans

Marian Himstedt, Sabrina Keil, Sven Hellbach and Hans-Joachim Böhme

***Abstract*—Mobile robots in industrial environments require accurate maps in order to perform navigation and service tasks. This paper presents a SLAM framework consisting of different optimization components aiming at building very accurate maps. We incorporate high-level feature extractors in the front-end supplying priors for data association. Due to perceptual aliasing 2D laser representations are likely to cause false loop closure detections which is robustly solved by state-of-the-art graph optimization techniques in the back-end. A final post-processing step generates highly accurate maps using an advanced sensor model incorporating specific characteristics of laser range finders. The presented framework is evaluated on datasets obtained from a typical industrial environment. The final map accuracy is estimated given ground truth measurements of the traversed environment.**

I. Introduction

The autonomous operation of mobile robots in industrial environments requires the precise position and orientation of the platform with respect to a global reference frame. Setting artificial landmarks such as visual markers can easily solve this problem, however, requires the environment to be modified. Prior maps built with onboard sensors, in contrast, enable robots to navigate independently of the presence of markers. Providing the path of the area traversed is known, a map can easily be built. For most of the cases these paths are not available respectively hard to obtain at high accuracy for indoor environments. If both, map and path, are unknown, the robot has to concurrently maintain estimates about its position as well as the traversable environment which is well known as the Simultaneous Localization and Mapping (SLAM) problem. This paper presents a SLAM framework enabling to build highly accurate maps using laser range finders which is illustrated by Figure 1. This includes a front-end providing spatial relations of robot poses by means of local motions and loop closures. This information is passed to a back-end that maintains pose relations and estimates the path travelled by the robot. A joint pose and map optimization is carried out afterwards given the estimated trajectory. The presented framework utilizes g2o [1], a generic graph optimization back-end, which is widely used among robotics and computer vision. Particularly optimization based approaches to the SLAM problem are quite actively researched. Hence there exist a large number of previous work which is outlined in excerpts. Olson et al. introduces an efficient method to pose graph optimization using gradient descent [2]. Grisetti et al. presented a tree based implementation, coined TORO, which explicitly bounds the graph optimization to the size of the map instead of the length of the trajectory [3]. In [4] Kretzschmar and Stachniss suggest to further reduce the complexity of pose graphs by means of information theory. Blanco et al. proposed a generic interface to hybrid metric-topological SLAM building a graph of occupancy grid based submaps which is well suited for mapping large-scale environments [5]. Metric-based SLAM systems, such as RBPF [6], are supplemented by place recognition methods as, for instance, FAB-MAP [7]. An incremental solution enabling optimization based SLAM for online applications is given by iSAM [8]. The key idea of this approach is that only a small subset of the variables in a factor graph need to be updated for incremental operation. Kaess et al. further extended their algorithm enabling incremental variable reordering and relinearization using a Bayes tree [9]. In [9] it is demonstrated that iSAM outperforms other state-of-the-art approaches as HOG-MAN [10] and Spa2D [11] on real-world datasets. However, our framework rather focusses on building an accurate map which does not neccessarily have to be performed online as datasets are rather batch processed for this purpose.

The optimization based SLAM approaches mentioned above provide substantial results in terms of accuracy as they seek to find the optimal solution to the given graph representation according to associated constraints. However it is assumed that all loop closure detections are correct which poses a high demand for data association in the front-end. Geometric consistency checks as commonly found in visual SLAM systems, as for example described in [12], can minimize the number of false detections but cannot generally avoid them. This is because some places can hardly be distinguished due to perceptual aliasing, particularly for 2D laser scans in the presence of many repetitive structures as, for instance, in industrial environments. In addition to that, expensive data association techniques are required that might also reject true loop closures due to more pessimistic evaluations. False constraints on the other side are likely to cause divergence in graph optimization which cannot be suffiently mitigated by robust methods such as pseudo Huber error functions as shown in [13]. In [14] Sünderhauf and Protzel proposed a robust optimization method enabling the back-end to modify the pose graph by switching loop closure constraints. This allows quite simple data association techniques in the front-end passing a higher number of loop closure candidates and associated confidences to the back-end which is able to disable

All authors are with the Artificial Intelligence Group, University of Applied Sciences, Dresden, Germany. This work was supported by ESF grant number 100076162. E-mail: himstedt@htw-dresden.de

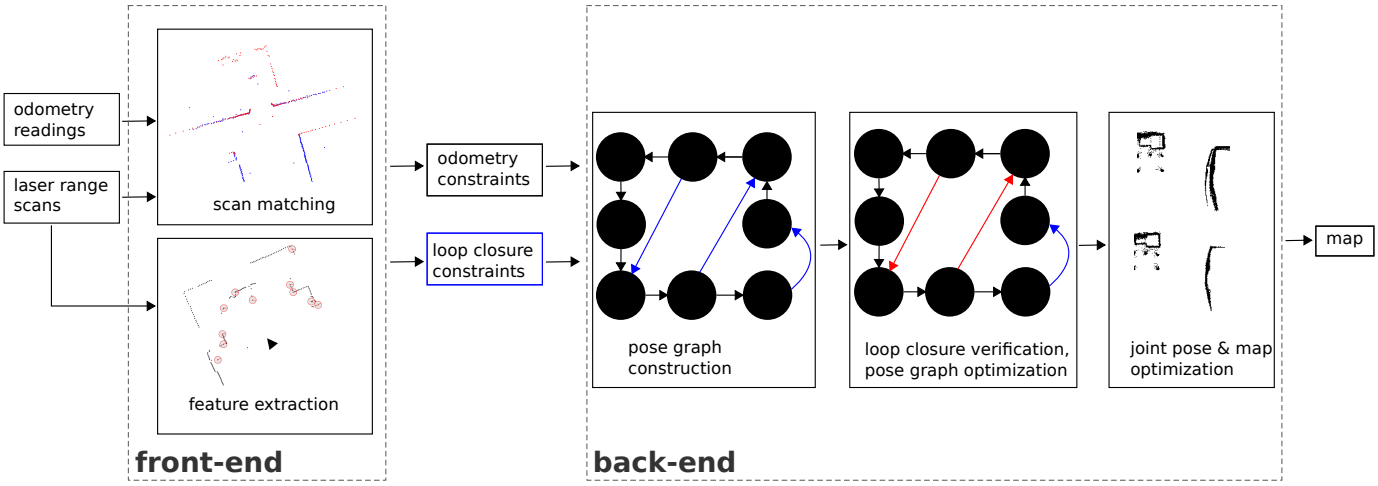

Figure 1. Framework overview.

wrong constraints. As this technique is incorporated in the presented framework, a more detailed description is given in the remainder of this paper.

From the robust back-end it is expected to obtain a topological consistent pose graph. The final map is then estimated given this representation. As demonstrated by Ruhnke et al. in [15] it is advantageous to model the physics of a laser beam in order to maximize the local accuracy of maps. This specifically addresses the range and the incident angle of a beam. A highly accurate map representation can be obtained by jointly optimizing the beam measurements with respect to their characteristics, their local sorroundings and the origin sensor poses [15]. This paper shows the benefit of that idea with the specific application of mapping industrial environments by mobile robots using only 2D laser range finders and wheel odometry.

The remainder of this paper is organized as follows. The Sections II and III describe the framework's front- and back-end with their components. We present experimental results in Section IV before concluding in Section V.

II. The Mapping Front-End

This section describes the front-end of our mapping framework. It provides an initial estimate about the successive robot poses. In addition to that the front-end is responsible for recognizing previously observed places and thus passes loop closure candidates to the back-end. This is done by extracting features from laser range scans which are matched to those obtained from the previous scans.

A. Initial estimate

The relative transformations between successive robot poses of the trajectory is given by odometric measurements. Due to wheel slip these estimates are likely to drift quickly. We use laser scan matching to correct the position estimates obtained from the odometry. A point-to-line metric based ICP algorithm is applied as presented in [16].

B. Feature extraction

We use Fast Laser Interest Region Transform (FLIRT) [17] which is inspired by prior work on scale invariant point feature detectors in computer vision. FLIRT considers the range data of a laser as a one dimensional curve which is mapped into a multi-scale representation. Hence we obtain curves for all scales which are smoothed by varying Gaussian kernels. The smoothing kernels are normalized in order to be invariant to the sampling density. Local extrema are detected for each scale. The mathematical derivation of this is given in [18]. Finally we obtain a set of interest points as local maxima with gradients above a certain threshold. These points typically refer to corners in the 2D representation of the scan.

The detected interest points are further assigned descriptors in order to associate them with previously observed ones. Similiar to common feature detectors in computer vision Tipaldi et al. proposed feature descriptors capturing local surroundings of interest points [17] which enables to recognize observed features in subsequent scans. Range measuring sensors such as LRFs give explicit information about free and occupied space covered by the sensor's field of view (FOV). Hence it is advantageous to incorporate this for the descriptors. A polar tesselation encoding the occupancy probabilities around each interest point is built. This is similiar to occupancy grid mapping, however we only generate high-resolution grids around the interest points instead of describing the entire area covered by the laser scan. As FLIRT interest points are highly distinctive and do not assume specific geometric primitives, they are well suited for a number of environment types that are not featureless (as for example long corridors). More details on the feature detector and descriptor can be found in [17].

C. Detection of loop closures

The most important requirement of a SLAM system is its ability to detect and incorporate information about places that have already been visited which are referred to as loop closures. These enable to reduce the accumulated pose un-

certainty increasing over time. Substantial research addressing loop closure detection in 2D range scans has been carried out and can be divided into grid map and feature based approaches.

Grid map based approaches usually do not scale well with increasing map sizes as they encode a lot of free space. This is particularly the case for approaches based on Rao-Blackwellized particle filters (e.g. [6]) since each particle holds an individual map of the entire trajectory. Feature based approaches on the other side often assume specific structures in environments such as corners which hampers their use in structureless environments. However, industrial environments which are the special focus of this paper typically consist of fine structures originated by objects such as shelves or machines. These structures are well taken into account by FLIRT interest points extracted from each laser scan. These are matched to the features of the previous scans using the symmetric χ^2 metric and a nearest neighbour strategy. The set of corresponding features is passed to a RANSAC based geometric consistency check. Each pair of interest points having a distance in the descriptor space below a threshold are threated as putative correspondences. A minimum set of two pairs is randomly drawn from the correspondence set. The RANSAC iteration is then carried out as follows. The spatial distances of the putative matches are computed. If the offset of these distances is below a threshold a hypothesis is generated by estimating the transformation between these two points. This transformation is applied to all observed features in order to project these into the reference scans' coordinate frame. Hence, each observed feature point is assigned the closest corresponding feature point of the reference scan. The squared distances of all pairs are summed which serves as the matching score for the two scans. Only those pairs having a distance below a threshold are added to the inlier set. The outlined procedure is repeated as common in RANSAC based data association. A loop closure constraint is generated provided the remaining set of inliers is above a threshold t_{min}. The value of t_{min} highly depends on the robustness of the optimization back-end, specifically on how well it handles data assocation errors.

For performance reasons a lot of SLAM front-ends do not consider all places of the trajectory for data association. For instance, the implementation Karto which uses graph based optimization as proposed in [11] defines a fixed search radius around the current pose to reduce the operation time. However, this is crucial for mapping large scale environments as pose priors might deviate significantly from the true pose due to accumulated odometric errors. Hence this radius should rather be set dynamically according to the pose uncertainty. Also Grisetti et al. suggest to limit the number of places to be considered in the recognition due to performance reasons and the risk of wrong associations. Since our framework post-processes datasets we are not necessarily affected by performance limitations. Based on robust optimization back-ends such as proposed by [14] we are able to successfully identify wrong loop closure constraints which is extensively explained in Section III.

III. The optimization back-end

Thanks to the front-end we are given an initial graph of robot poses and relations expressing spatial constraints between those. The optimization of this graph is the task of the back-end. The remainder of this section briefly introduces pose graph SLAM, explains how to handle false loop closure detections and the final map is built.

A. Pose Graph SLAM

Providing the navigation of a mobile robot is carried out in a 2D space, its state vector can be described by $\mathbf{x} = (x, y, \phi)^T$. Pose graph SLAM only optimizes robot poses $\mathbf{x_i}$ of a given trajectory omitting optimization of landmarks respectively scan points. The graph consists of vertices given by the poses $\mathbf{x_i}$ and edges between the poses $\mathbf{x_i}$ and $\mathbf{x_j}$. The action $\mathbf{u_i} = \Delta(x, y, \phi)$ is carried out in order to get from the state $\mathbf{x_i}$ to $\mathbf{x_{i+1}}$ and is incorporated according to a motion model:

$$\mathbf{x_{i+1}} \sim \mathcal{N}(f(\mathbf{x_i}, \mathbf{u_i}), \Sigma_i) \tag{1}$$

Without loss of generality we can describe the motion of loop closings detected for the poses $\mathbf{x_i}$ and $\mathbf{x_j}$ by $\mathbf{u_{ij}}$, hence we can postulate the following about state $\mathbf{x_j}$:

$$\mathbf{x_j} \sim \mathcal{N}(f(\mathbf{x_i}, \mathbf{u_{ij}}), \Lambda_{ij}) \tag{2}$$

Given all states X and all actions U we aim at finding the maximum a posteriori estimate of robot poses X^* for the joint probability distribution

$$X^* = \underset{X}{\operatorname{argmax}}\, P(X|U) \tag{3}$$

We can account for this by the following factorization:

$$P(X|U) \propto \prod P(\mathbf{x_{i+1}}|\mathbf{x_i},\mathbf{u_i}) \cdot \prod_{ij} P(\mathbf{x_j}|\mathbf{x_i},\mathbf{u_{ij}}) \tag{4}$$

with $P(\mathbf{x}_{i+1}|\mathbf{x}_i, \mathbf{u}_i)$ expressing odometry constraints and $P(\mathbf{x}_j|\mathbf{x}_i, \mathbf{u}_{ij})$ the loop closure constraints. According to [19] we can express the objective function 3 as a nonlinear least squares optimization problem that can be solved using common methods such Gauss-Newton or Levenberg-Marquardt:

$$X^* = \underset{X}{\operatorname{argmin}} \sum_i \left\| e_i^{odo} \right\|^2_{\sum_i} + \sum_{ij} \left\| e_{ij}^{lc} \right\|^2_{\Lambda_{ij}} \tag{5}$$

with $e_i^{odo} = f(\mathbf{x_i}, \mathbf{u_i}) - \mathbf{x_{i+1}}$ and $e_{ij}^{lc} = f(\mathbf{x_i}, \mathbf{u_{ij}}) - \mathbf{x_j}$. An extensive derivation of this is given by [13].

B. Robust optimization

In [20] Tipaldi et al. demonstrated the robustness and high repeatability of FLIRT interest points in a SLAM framework. However the authors used TORO [3] as optimization back-end which is not robust in the presence of false loop closure detections. This is a significant drawback for environments with a multitude of repetitive structures that can be hardly distinguished by 2D laser scans. A sliding window limiting

the pose search space to a local region around the current estimate is proposed to minimize this problem. However, it hampers the application in environments with large loops and bad prior pose estimates as obtained, for instance, by wheel odometers.

Conventional least squares based optimization approaches to the SLAM problem keep the structure of the supplied pose graph fixed assuming all loop closure constraints to be correct. Sünderhauf and Protzel proposed Switchable Constraints tackling the optimization by a modified objective function. Their work uses factors in the graphical model expressing switchable loop closure constraints. Based on that the topology of a graph is not fixed, but made subject to optimization as well. Loop closures expressed as switch variables s_{ij} can be disabled in this way. The contribution of a loop closure to the optimization can be incorporated by its initial value γ_{ij} and a corresponding covariance Ξ_{ij}. These estimtates can, for instance, be given in terms of a degree of belief by a place recognition system of the front-end. These switch priors are neccessary to avoid all loop closures being switched off by the optimizer as shown in [14]. In order to include the switchable constraints in the optimization the objective function (Eq. 5) is modified as follows:

$$X^*, S^* = \underset{X,S}{\operatorname{argmin}} \sum_i \left\| e_i^{odo} \right\|^2_{\sum_i} + \sum_{ij} \left\| e_{ij}^{slc} \right\|^2_{\Lambda_{ij}} + \sum_{ij} \left\| e_{ij}^{sp} \right\|^2_{\Xi_{ij}}$$

with $e_{ij}^{slc} = \Psi(s_{ij}) \cdot (f(\mathbf{x_i}, \mathbf{u_{ij}}) - \mathbf{x_j})$ expressing the switched loop closure constraints and $e_{ij}^{sp} = \gamma_{ij} - s_{ij}$ the switch priors. The switching function Ψ maps the continous input numbers s_{ij} to the interval $[0, 1]$. The loop closure constraint s_{ij} is switched off by $\Psi(s_{ij}) \approx 0$. The optimization process can be influenced by the choice of the switch function Ψ, the switch priors γ and their covariances Ξ as explained in detail in [13].

C. Map building

Sparse surface adjustment (SSA) is a joint optimization problem aiming at finding optimal settings of robot poses and laser measurements. This method was presented by Ruhnke et al. in [15] and is very similiar to Sparse Bundle Adjustment (SBA) in computer vision. SBA optimizes a set of camera poses and 3D points of an image sequence by minimizing over the points' reprojection errors. Similiarly SSA optimizes robot poses and laser points, however SBA requires point-to-point and SSA, in contrast, point-to-surface correspondences in the data association. It is further assumed that the environment consists of smooth surfaces which is very common for man-made structures. A modified sensor model explicitely accounts for uncertainty in distance measurements of laser range finders that mainly occur due to incident angles and distance varying local surface characteristics. This is done by describing the laser scan as a set of surface tangents with each representing one laser beam. The tangents are modelled as Gaussians with the mean μ_{ik} centred at the laser beam k of robot the pose i and the covariance estimated $\sum_{ik}$ based on the surrouding points. Surfaces are smoothly moved along their tangential direction and more rigidly along their normal directions facing the robot pose. The joint optimization problem of robot poses X and surface patches M is formulated as follows [15]:

$$X^*, M^* = \underset{X,M}{\operatorname{argmin}} \sum_i \left\| e_i^{odo} \right\|^2_{\sum_i} + \sum_{m,n} e_{lm}^{surf} + \sum_{i,k} e_{ik}^{meas} \quad (6)$$

with e_{mn}^{surf} expressing the minimization term for the tangential and normal error arising for the surface patches m and n. The term e_{ik}^{meas} ensures that each laser beam k is assigned to a robot pose i. A more extensive derivation of this can be found in [15].

IV. Experiments

In order to evaluate the presented framework a number of experiments were carried out. For this purpose we manually steered a mobile robot through a warehouse capturing laser range scans and wheel odometry. The following section briefly introduces the mobile platform used for the experiments and discusses the results obtained. First the necessity of a robust optimization back-end is demonstrated. The second part shows the final mapping accuracy achieved with the presented framework in a typical industrial environment.

A. Platform

A Scitos G5 platform developed by Metralabs GmbH Germany is used (see Figure 2). It is equipped with a rig of four cameras, two laser range finders (Hokuyo URG04-LX, SICK S300), a TOF camera (PMD Camcube 3.0) and wheel odometry. Only the forward-facing SICK S300 is used for map building.

Figure 2. A Scitos G5 navigating in a warehouse.

B. Contribution of a robust back-end

Even though FLIRT interest points are very distinctive the number of false loop closure detections is high. This is mainly due to perceptual aliasing arising from the limited scene representation of 2D laser scans. Geometric consistency checks cannot prevent this in all cases since the environment is rich of repetitive structures such as shelves and boxes. Figure 3 illustrates the results of the pose graph optimization emphasizing the importance of a robust back-end. We used the Switchable Constraints [14] implementation, coined vertigo, with a linear switch function. Furthermore we made use of the generic graph optimization back-end g2o [1]. Both implementations are obtained from the openslam[2] platform.

C. Mapping performance

Given the optimized pose graph as shown in Figure 4 a final map is built by concurrently optimizing robot poses and laser measurements as explained in Section III-C. It can be clearly seen that pure pose graph optimization is not sufficient to get accurate and consistent maps. The map consistency is significantly improved by the joint optimization of robot poses and laser measurements.

In order to estimate the final map accuracy a second experiment was carried out in a subarea of the warehouse which is illustrated by Figure 2. The robot was steered two loops in that subarea. Ground truth was obtained by measuring distances $L_1 ... L_6$ between salient points using a tape measure (see also Figure 5a). The distances Δ between these salient points were also manually estimated in the final map obtained after optimization (see Figure 5c). The results are shown in Table I. The differences Δ are supplemented by the mean μ and variance Var over all differences. Note that GT determine the actual ground truth distances measured. The values Δ, in contrast, are the differences obtain from the distances that were manually measured on the final map and the GT measurements. The mean $\mu(L)$ is around 3cm, the high variance $\mathrm{Var}(L)$ is mainly achieved due to the rather low distance for L_4. Similiarly to [15] we further estimated the entropy of the maps shown in Figure 5b and 5c respectively which are given in Table II for ICP, pose graph SLAM (pose only) and joint pose and laser measurement optimization (SSA). The optimization of laser measurements helps minimizing that points are spread around objects which results in a lower entropy. As we do not aim to reduce the actual information (here obstacles on the height of the laser range finder), a lower boundary determining the optimal representation should be approached.

	GT [mm]	**Δ[mm]**
L_1	1490.0	49.24
L_2	762.0	47.05
L_3	791.0	40.82
L_4	650.0	8.34
L_5	892.0	39.48
L_6	1206.0	20.04
$\mu(L)$	-	**34.16**
$\mathrm{Var}(L)$	-	**26.64**

Table I
RESULTS OF EXPERIMENT 2.

ICP	**Pose only**	**SSA**
0.186	0.132	0.102

Table II
ENTROPY ON MAPS OF EXPERIMENT 2.

V. CONCLUSIONS

This paper presented a framework consisting of state-of-the-art algorithms in graph based SLAM. We combined existing methods to achieve an overall solution which is able to generate maps at high accuracy using laser range scans. The importance of each component for achieving this final goal is extensively demonstrated for a complex industrial environment, more precisely a warehouse, which poses the main contribution of this work. The robust pose graph optimization was shown to be essential in the presence of a multitude of repetitive structures which naturally occur in 2D range scans for this type of environment. The FLIRT interest points were shown to be beneficial for loop closure detections. The combination with a robust optimization back-end allows us to tackle environments at much larger scales. Finally incorporating a post-optimization of robot poses and laser measurements brings us significantly closer to more local map accuracy. We evaluated the overall accuracy of the map that can be achieved by means of ground truth comparisons obtained for a specific scene in the warehouse. These high-resolution maps are very contributive for the autonomous operation of mobile robots in industrial settings. This specifically addresses the localization in such environments hampering the setting of artificial markers. It further enables precise positioning in order to get close to surrounding objects or charging stations. Most common environments in mobile robotics are represented by occupancy grid maps serving as input for path planning, obstacle avoidance and localization. In order to achieve optimal results it is recommended to keep grid sizes small ensuring less information loss. However, holding maps of large-scale environments at fine resolution is computationally expensive. Hence, methods as presented by Einhorn et al. [21] enable to manage occupancy grid maps with adaptive grid sizes. In this way large free space can be described by larger grid cells, whereas fine local structures can be kept at high resolution. We will incorporate this technique in future work in order to enable more autonomy for mobile robots in industrial environments by achieving more robust navigation and positioning.

ACKNOWLEDGMENT

The authors highly acknowledge prior work on robust graph optimization by Sünderhauf and Protzel [14], surface adjustment by Ruhnke et al. [15] as well as laser scan based

[2]http://www.openslam.org

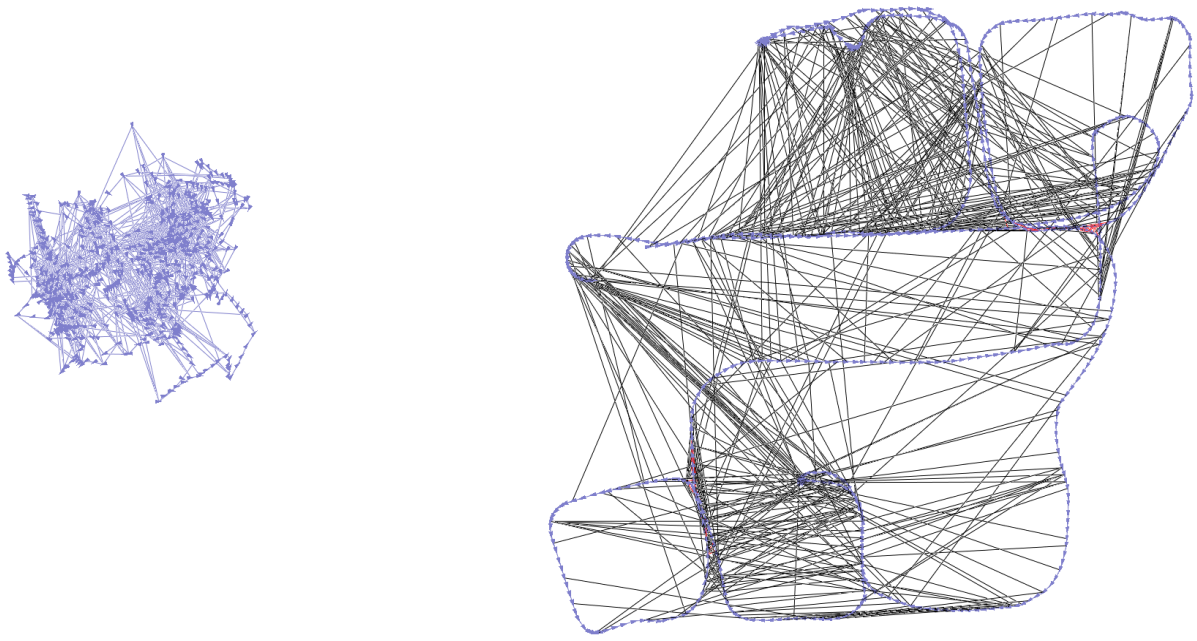

(a) Diverged optimization result without robust back-end.

(b) Consistent pose graph using Switchable Constraints. Loop closure constraints s_{ij} having switch values $\Psi(s_{ij}) > 0.999$ are enabled and plotted red, all others are disabled and plotted black. It can be clearly seen that a high number of false loop closures is correctly identified.

Figure 3. Results of the pose graph optimization using conventional (a) and robust back-ends (b) respectively.

feature extraction by Tipaldi et al. [17], particularly for making implementations publicly available.

REFERENCES

[1] R. Kummerle, G. Grisetti, H. Strasdat, K. Konolige, and W. Burgard, "g2o: A general framework for graph optimization," in *ICRA*, Shanghai, 2011.

[2] E. Olson, J. Leonard, and S. Teller, "Fast iterative optimization of pose graphs with poor initial estimates," 2006, pp. 2262–2269.

[3] G. Grisetti, S. Grzonka, C. Stachniss, P. Pfaff, and W. Burgard, "Efficient estimation of accurate maximum likelihood maps in 3d," San Diego, CA (USA), 2007, pp. 3472–3478.

[4] H. Kretzschmar and C. Stachniss, "Information-theoretic compression of pose graphs for laser-based slam," vol. 31, pp. 1219–1230, 2012.

[5] J.-L. Blanco, J.-A. Fernandez-Madrigal, and J. Gonzalez, "A new approach for large-scale localization and mapping: Hybrid metric-topological slam," in *Robotics and Automation, 2007 IEEE International Conference on*, 2007, pp. 2061 –2067.

[6] G. Grisetti, C. Stachniss, and W. Burgard, "Improving grid-based slam with rao-blackwellized particle filters by adaptive proposals and selective resampling," in *Robotics and Automation, 2005. Proc. of the 2005 IEEE International Conference on*, Apr. 2005, pp. 2432 – 2437.

[7] M. Cummins and P. Newman, "FAB-MAP: Probabilistic Localization and Mapping in the Space of Appearance," *The International Journal of Robotics Research*, vol. 27, no. 6, pp. 647–665, 2008.

[8] M. Kaess, A. Ranganathan, and F. Dellaert, "iSAM: Incremental smoothing and mapping," *IEEE Trans. on Robotics (TRO)*, vol. 24, no. 6, pp. 1365–1378, Dec. 2008.

[9] M. Kaess, H. Johannsson, R. Roberts, V. Ila, J. Leonard, and F. Dellaert, "iSAM2: Incremental smoothing and mapping using the Bayes tree," *Intl. J. of Robotics Research (IJRR)*, vol. 31, pp. 217–236, Feb. 2012.

[10] G. Grisetti, R. Kummerle, C. Stachniss, U. Frese, and C. Hertzberg, "Hierarchical optimization on manifolds for online 2d and 3d mapping," in *Robotics and Automation (ICRA), 2010 IEEE International Conference on*, 2010, pp. 273–278.

[11] K. Konolige, G. Grisetti, R. Kümmerle, W. Burgard, B. Limketkai, and R. Vincent, "Efficient sparse pose adjustment for 2d mapping," in *Proc. of the IEEE/RSJ Int. Conf. on Intelligent Robots and Systems (IROS)*, Taipei, Taiwan, October 2010.

[12] D. Galvez-Lopez and J. D. Tardos, "Bags of binary words for fast place recognition in image sequences," *IEEE Transactions on Robotics*, vol. 28, no. 5, pp. 1188–1197, October 2012.

[13] N. Sünderhauf, "Robust optimization for simultaneous localization and mapping," Ph.D. dissertation, 2012.

[14] N. Sünderhauf and P. Protzel, "Towards a robust back-end for pose graph slam," in *Robotics and Automation (ICRA), 2012 IEEE International Conference on*, may 2012, pp. 1254 –1261.

[15] M. Ruhnke, R. Kümmerle, G. Grisetti, and W. Burgard, "Highly accurate maximum likelihood laser mapping by jointly optimizing laser points and robot poses," in *Proc. of the IEEE Int. Conf. on Robotics & Automation (ICRA)*, 2011.

[16] A. Censi, "An ICP variant using a point-to-line metric," in *Proceedings of the IEEE International Conference on Robotics and Automation (ICRA)*, May 2008.

[17] G. Tipaldi and K. Arras, "Flirt - interest regions for 2d range data," in *Robotics and Automation (ICRA), 2010 IEEE International Conference on*, 2010, pp. 3616 –3622.

[18] R. Unnikrishnan and M. Hebert, "Multi-scale interest regions from unorganized point clouds," in *Workshop on Search in 3D (S3D), IEEE Conf. on Computer Vision and Pattern Recognition (CVPR)*, June 2008.

[19] M. W. M. G. Dissanayake, P. Newman, S. Clark, H. F. Durrant-whyte, and M. Csorba, "A solution to the simultaneous localization and map building (slam) problem," *IEEE Transactions on Robotics and Automation*, vol. 17, pp. 229–241, 2001.

[20] G. D. Tipaldi, M. Braun, and K. O. Arras, "Flirt: Interest regions for 2d range data with applications to robot navigation," in *Proceedings of the International Symposium on Experimental Robotics (ISER)*, Dehli, India, 2010.

[21] E. Einhorn, C. Schroter, and H. Gross, "Finding the adequate resolution for grid mapping - cell sizes locally adapting on-the-fly," in *Robotics and Automation (ICRA), 2011 IEEE International Conference on*, 2011, pp. 1843–1848.

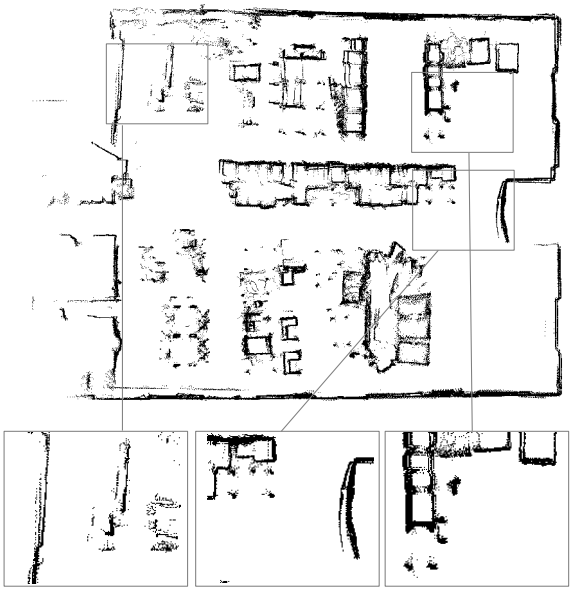

(a) Initial input obtained from pose graph SLAM. Some walls appear twice in the map. Fine local structures are not accurately captured and seem spread around objects.

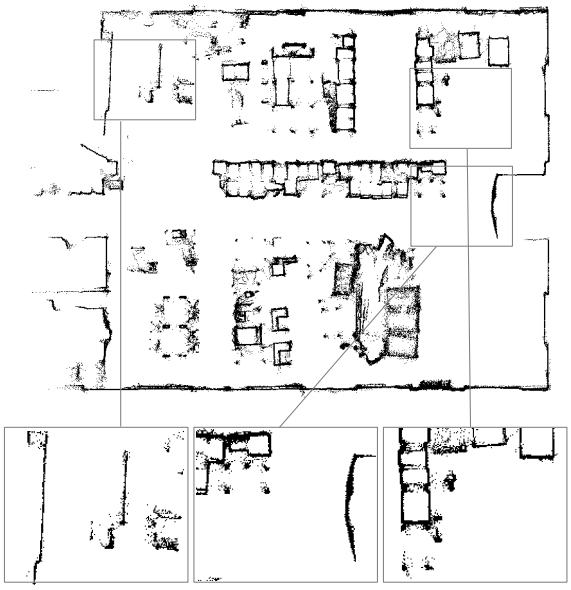

(b) Results obtained through joint optimization of poses and laser points using Sparse Surface Adjustment. Laser measurements are less spread around objects. The effect of double appearing walls and structures is significantly minimized.

Figure 4. Map building given a prior graph obtained by pose graph SLAM. Note that the angular resolution of the laser range finder (SICK S300) used for this experiment is high resulting in a much more dense scan containing 541 measurements. The SICK LMS which is used for many publibly available datasets in contrast only obtains 181 laser measurements. This difference becomes evident in the final map's point density. It is also obvious that large continous surface patches are well optimized, whereas very fine local structures such as lattice boxes seem less qualitively incorparated. This is due to the fact that these surfaces are more challenging for the data association and surface based optimization.

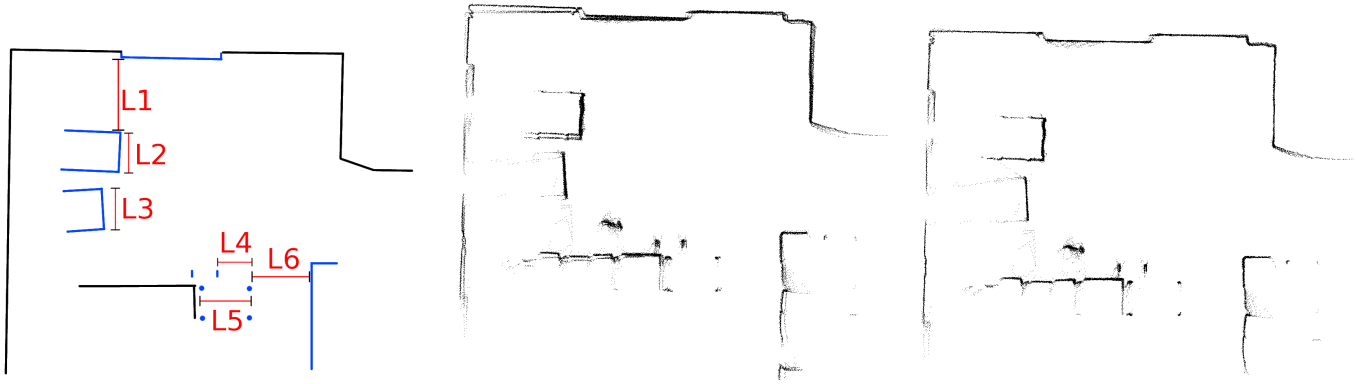

(a) Ground truth map

(b) Map built using the initial pose graph

(c) Final map obtained after joint pose and laser measurement optimization.

Figure 5. Ground truth measurements as references and final maps obtained for the scene shown in Figure 2.